



Fabrication and Characterizations of Metallic Mg Containing PMMA-Based Partially Degradable Composite Bone Cements

Xiao Lin^{1,2} · Adrian Chan³ · Xiao-Xiao Tan⁴ · Hui-Lin Yang^{1,2} · Lei Yang^{1,2}

Received: 14 August 2018 / Revised: 12 September 2018 / Published online: 1 November 2018
© The Chinese Society for Metals and Springer-Verlag GmbH Germany, part of Springer Nature 2018

Abstract

Inadequate strength at the bone/cement interface is one of the main drawbacks of poly(methylmethacrylate) (PMMA) bone cement in the current orthopedic surgeries. In the present work, a partially degradable PMMA/Mg composite bone cement (PMC) was developed for enhancing the bone/cement interfacial strength, which is proposed to be accomplished by increasing the osteo-conductivity of PMMA and enhancing the mechanical interlocking between bone tissue and the porous PMMA surface formed by the degradation of Mg on the surface of the cement. PMCs were prepared with various concentrations of Mg particles with different sizes and alloy compositions. The effects of Mg particle size, composition and content on the injectability, mechanical and degradation properties, and biocompatibility of PMCs were evaluated. The results show that these parameters affected the properties of the PMCs simultaneously. The good injectability and compressive strengths of PMMA were preserved, while the compatibility to osteoblasts was enhanced when adding Mg particles in a proper manner. The PMCs degraded at the surface with time and formed porous surface structures in the physiological environment, while maintaining the original compressive strengths. This preliminary study shows that the PMC is promising for minimally invasive orthopedic surgery; however, it still requires to be optimized and evaluated in the future.

Keywords Biomaterials · Composite · Magnesium · Poly(methylmethacrylate) · Bone cement · Kyphoplasty

1 Introduction

Metallic magnesium (Mg) and its alloys have recently been designed as biodegradable materials, with tunable degradation rate in vivo [1, 2], primarily for orthopedic applications. The osteo-bioactivity and other biological activities of Mg have been uncovered [1, 3–6]. For example, Feng et al. revealed strong antibacterial effects of

pure Mg against *Staphylococcus aureus* [5]. And the relatively high initial degradation rate of Mg and its alloys could be controlled by various surface coating strategies [7–12]. Recent clinical studies have revealed the great translational potential of Mg and its alloys as screws for hand-and-wrist fractures [13], or as screws for the fixation of vascularized bone graft in treatment of osteonecrosis of the femoral head [14]. In addition to being applied in the form of bulk devices, Mg alloys could also be used as additives to develop composite materials with handling, mechanical, degradation and/or biological properties superior to Mg and other components of the composite [15–19]. For example, the addition of AZ31 fibers in the PLGA matrix effectively improved the tensile strength and elongation of PLGA, as well as the adherence and proliferation of MC3T3 osteoblasts on the PLGA matrix [17].

The injectable and in situ setting implants own numerous advantages over pre-shaped implants, especially for the applications in the minimally invasive orthopedic surgery (MIOS). Poly(methylmethacrylate) (PMMA)-based bone cements, as a kind of injectable and in situ setting implants,

Available online at <http://link.springer.com/journal/40195>

✉ Lei Yang
leiy@suda.edu.cn

- ¹ Orthopaedic Institute, Soochow University, Suzhou 215006, China
- ² Department of Orthopaedics, The First Affiliated Hospital of Soochow University, Suzhou 215006, China
- ³ Waterloo Institute for Nanotechnology (WIN), University of Waterloo, 200 University Ave West, Waterloo, ON, Canada
- ⁴ School of Materials Engineering, Shanghai University of Science and Engineering, Shanghai 201620, China

have been widely used in current orthopedic surgeries, including arthroplasty, treatments of femoral head osteonecrosis and spinal degenerative diseases [20, 21]. Compared with other injectable systems, PMMA has higher mechanical strength and is more suitable for load-bearing applications, such as percutaneous kyphoplasty (PKP). Nevertheless, the need for improving PMMA rises since the increasing number of clinical cases indicates the risks of inadequate bone/cement interfacial strength, causing the instability of the interface or even failure of the bone bonding to cement [22–25]. The inadequate interfacial strength was attributed to the lack of osseointegration and biodegrading ability of PMMA [26–28].

The biodegradable Mg is proposed to modify the PMMA bone cement by preparing partially degradable PMMA/Mg composite bone cement (PMC), aiming at improving the osseointegration of PMMA bone cement by increasing the osteo-conductivity of PMMA, and enhancing the physical interlocking between the bone tissue and the porous PMMA surface formed by the degradation of Mg on the surface. Additionally, the degradation of Mg would release Mg element in the form of ions, which is essential for bone development and metabolism [3]. The antibacterial capabilities would also be enhanced through Mg degradation, which could reduce the rate of implant-related infection that would lead to undesirable consequences [29].

In the present work, PMCs were prepared with various concentrations of Mg particles of different sizes and alloy compositions. Several properties that strongly influenced the applications, including the injectability, mechanical properties, degradation properties and biocompatibility of the PMCs, were evaluated. The effects of Mg particle size, composition and content on these properties were revealed for further optimization of the PMCs.

2 Experimental

2.1 Materials Preparation

MENDEC[®]Spine (TECRES, Italy) PMMA bone cement for PKP surgery was used for the study. The PMMA/Mg composite bone cement (PMC) was prepared by mixing Mg particles with PMMA powder uniformly, followed by mixing with MMA monomer. In detail, 0.2 or 0.4 g of Mg particles was mixed with 2 g of PMMA powder. Then, 1 ml of MMA monomer was added in the mixed powder to form bone cement. Pure Mg (99.5 wt%) with particle diameter of 270–550 μm , 150–270 μm and 75 μm and ZK61 alloy (Zn: 6 wt%, Zr: 1 wt%) with diameter of 150–270 μm were used. The bone cement was designated as 0.2-Mg-L, 0.4-Mg-L, 0.2-Mg-M, 0.4-Mg-M, 0.2-Mg-S,

0.4-Mg-S and 0.2-ZK61, 0.4-ZK61. The “Mg-L,” “Mg-M” and “Mg-S” represent the Mg particles with diameter of 270–550, 150–270 and 75 μm , respectively. Before all the sample preparation, the Mg particles and MENDEC[®]Spine bone cement were kept at $(23 \pm 1)^\circ\text{C}$ for 2 h.

2.2 Injectability, Microstructure and Mechanical Properties

The bone cements were injected out of a disposable syringe at the dough time with a 50-N constant loading at $(23 \pm 1)^\circ\text{C}$. Injectability was defined as the weight percent of cement injected out of the syringe. For direct comparison, the injectability values of PMCs were normalized by the value of PMMA. The dough time was measured according to ISO5833: 2002 standard and determined by failure of the cement to stick to the surface of a surgically gloved probing finger.

The microstructure of the PMC was characterized by scanning electron microscopy (SEM, Quanta 250, FEI). Before SEM characterization, the samples were successively polished up to 2000 grit finish and then cleaned. All samples were coated with a thin 20Å layer of gold before the SEM observation.

The compressive test was performed according to ISO5833: 2002 standard with a mechanical tester (HY10000, HengYi, China) at 20 mm/min displacement rate. Cement cylinders of 6 mm diameter and 12 mm height were cast and pre-hardened in stainless-steel molds for the test.

2.3 In Vitro Degradation Test

Pre-hardened cement cylinders with a diameter of 6 mm and height of 12 mm were immersed in Hanks' solution, with a composition described in a previous work [30] and with the immersion ratio of 1.25 cm^2/mL at 37 $^\circ\text{C}$. The solution was refreshed every 2 days. The pH of solution and weight of the samples were monitored. The surface microstructure and compressive properties of the bone cement after immersion were characterized by SEM and compressive test (at displacement rate of 20 mm/min), respectively.

2.4 Cyto-Compatibility Test on Osteoblasts

MC3T3-E1 osteoblasts from the Type Culture Collection of Chinese Academy of Sciences (Shanghai, China) were selected for the cyto-compatibility tests. α -MEM (HyClone) with 10 vol% FBS (HyClone) and 1 vol% penicillin–streptomycin solution was used as the cell culture medium.

2.4.1 Indirect-Contact Cell Proliferation Test

The compatibility of degradation products of samples to osteoblasts was evaluated by culturing the osteoblasts with the sample extracts. For extracts preparation, the samples (15 mm diameter and 2 mm height) were immersed in 75% ethanol for 30 min for sterilization and then rinsed by PBS solution three times to remove the ethanol. After that, the samples were immersed in the cell culture media at an extraction ratio of 1.25 cm²/mL at 37 °C for 1 day. The supernatant was withdrawn and filtrated through a 0.22- μ m membrane filter (Millex-GP, Millipore) for cell tests. The cell culture media incubated at 37 °C for 1 day were set as the control group.

Osteoblasts were seeded onto the 96-well plate with 5000 cells/well in the presence of extracts for 1 and 3 days. After the prescribed times, cell culture mediums in each well was removed and the well was rinsed by 200 μ L PBS two times. Ten microliter CCK-8 (Dojindo Molecular Technologies, Inc.) mixed in 100 μ L PBS was then added to each well and incubated at 37 °C for 2 h. Then, the solution was transferred onto a new 96-well plate. The optical density (O.D.) of each well was measured on a micro-plate reader (Power Wave X, BioTek) at 450 nm. The O.D. value was positively correlated with the cell number in the well, reflecting the state of cell proliferation.

The pH value of extracts before each cell culture was measured by a pH meter (Lei-ci, China).

2.4.2 Direct-Contact Cell Test

For direct-contact cell test, samples with a diameter of 15 mm and thickness of 2 mm were used. Before the experiment, the samples were polished, cleaned and sterilized as described in Sect. 2.4.1. Then, the osteoblasts were seeded onto the samples at 10000 cells/cm² with cell culture media. The osteoblasts were cultured on these samples for 1 day. After culturing, the samples were gently rinsed with PBS and then fixed with 2.5% glutaraldehyde for 4 h and rinsed with PBS again. Then, the samples were dehydrated with a series of ethanol solutions (30, 50, 70, 80, 95 and 100% ethanol for 15 min each) and finally dried with the critical point drying equipment (CPD300, Leica) for SEM observation. All samples were coated with a thin 20 Å layer of gold before the SEM observation.

2.5 Statistical Analysis

Statistical analysis of the cell proliferation results was conducted by one-way analysis of variance. All the pairwise comparisons were made by the post hoc test of Turkey.

3 Results and Discussion

Previously, several studies on modified PMMA bone cement by incorporating bioactive or biodegradable additives (such as bioactive glass, hydroxyapatite, chitosan and MgO) in order to enhance its osseointegrative properties have demonstrated promising results [27, 28, 31–33]. Here, a new composite bone cement combining biodegradable Mg with PMMA was developed and this type of cement, to our knowledge, has not been reported before.

Figure 1 shows the microstructures of different PMCs after setting. The Mg particles were homogeneously distributed within the PMMA substrate for all the PMCs, which is beneficial for maintaining high mechanical strength and controlling the degradation behavior. The increased diameter from “small” Mg particles to “medium” ones (and ZK61 ones) and then to “large” PMCs will lead to the enlargement of pore size on the PMC surface formed after degradation of Mg particles. As expected, higher area fraction of Mg particles was found in the PMCs with higher Mg particle content.

The injection ratio (Fig. 2a) directly reflects the injectability of each PMC formulation, which is important for the PKP operation. Generally, the injectability of all the PMCs was lower than that of PMMA, which should be due to the increase in viscosity and setting rate of the cement paste after particle addition. Among the PMCs with pure Mg particles, the PMCs with “large” particles showed the worst injectability, followed by cements with “small” particles and cements with “medium” particles. The best injectability of PMC with “medium” particles should be due to its lowest viscosity and/or largest setting time. For PMCs with “large” and “medium” particles, the concentration of particles within PMCs had slight effect on the injectability. Differently, the concentration of “small” particles had significant influence on the injectability of cements. In spite of the similar size for “medium” Mg particles and ZK61 particles, the PMCs with ZK61 particles show injectability worse than those with “medium” Mg particles, which should be due to the difference in the surface physiochemical properties of the two particles when considering their different composition.

Mechanical strength of bone cement is critical for load-bearing applications, such as in PKP surgery. Different from the reported increase in compressive strengths for PMMA after addition of titania [34], the addition of Mg particles decreased the compressive strength of PMMA (Fig. 2b), which is consistent with what found for a PLLA/magnesium composite [19] and a PMMA/chitosan/HA composite bone cement [32]. For PMCs with 9 wt% and PMCs with 17 wt% Mg particles (except for 0.4-ZK61), there is a 10-MPa and a 20-MPa drop in

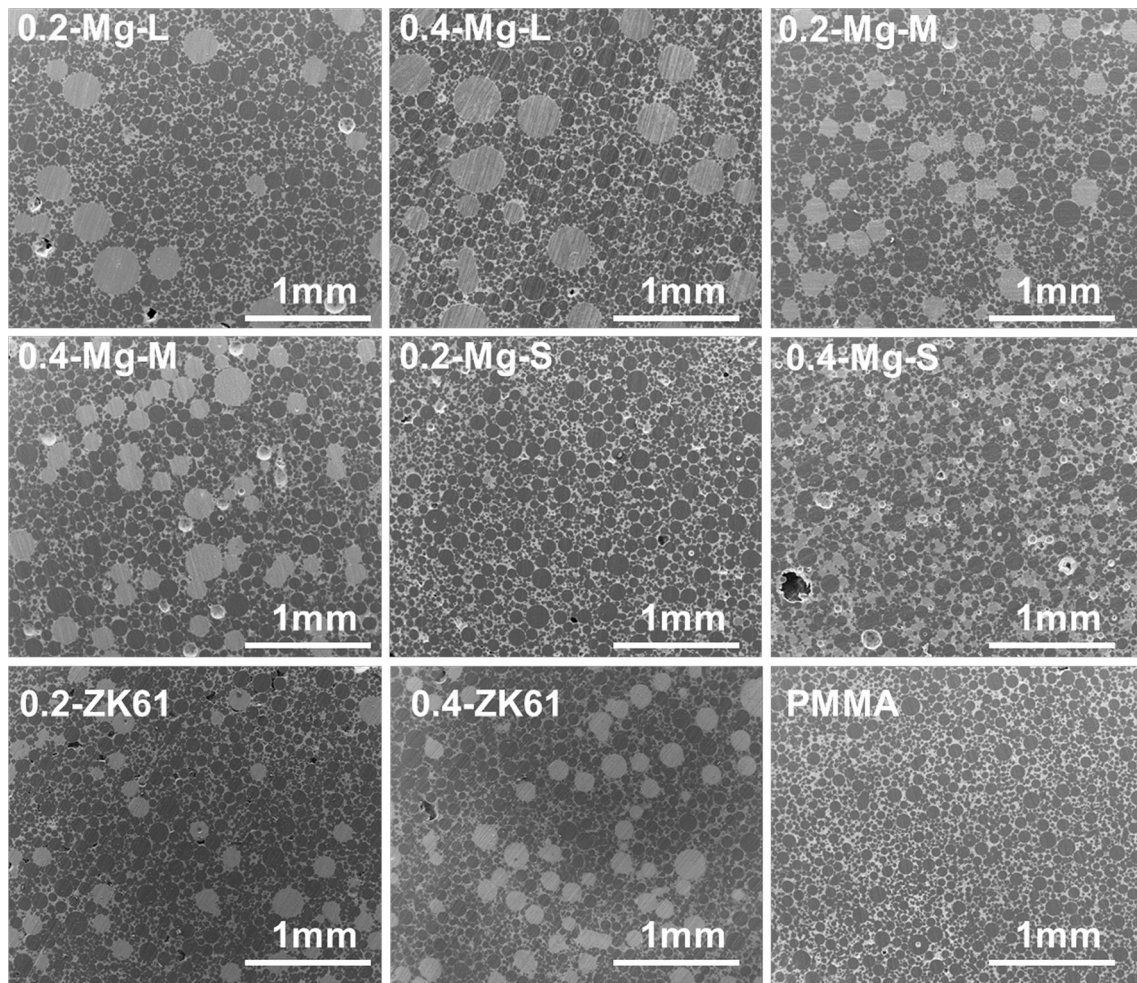


Fig. 1 SEM images of PMCs with various content of different Mg particles

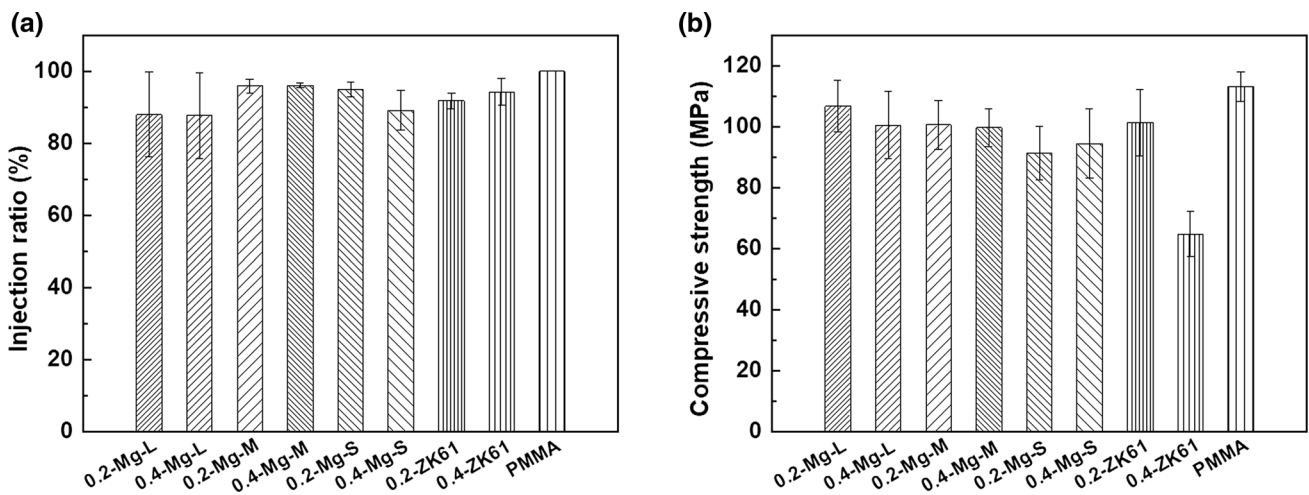


Fig. 2 Injection ratios **a** compressive strengths, **b** of different PMCs. Data are shown in mean \pm standard deviation

compressive strength, respectively. But the values are still high enough for most of the MIOSs. However, the 0.4-ZK61 PMC had a much larger drop in compressive

strength (down to ~ 60 MPa), which would limit its use when large load bearing is necessary. The decrease in compressive strengths is probably due to the relatively low

strength of Mg and weak bonding between Mg particles and PMMA substrate, as suggested by a previous work [19]. And the more significant decrease for 0.4-ZK61 is most likely due to the high amount of defects formed at the weakly bonded ZK61/PMMA interface. For the PMCs containing Mg particles, the compressive strength decreased with decreasing the size of Mg particle at the same content level, which should be due to the area increase in Mg/PMMA interface, which is the mechanically weak site. With increasing Mg content, the compressive strength of PMC decreased slightly for PMCs with “large” and “medium” Mg particles, while increased for PMC with “small” Mg particles. There should be a competition between the contributive effect of higher mechanical strength of Mg than PMMA and detrimental effect of weak Mg/PMMA interface on the overall mechanical strength of PMCs. When the contributive effect overwhelms the detrimental effect, the PMC will exhibit an increase in the mechanical strength, and vice versa.

As partly degradable implant, the degradation behavior of PMCs after implantation greatly influences their biological and mechanical properties. The degradation properties of the PMCs were characterized with a 2-month in vitro immersion test in Hanks' solution. Figure 3a shows the pH variation of Hanks' solution with PMMA–Mg composite cements, which reflects the degradation rate of PMCs at each time point [35, 36]. The pH values of PMC groups were always higher than those of PMMA group, indicating that the Mg particles at PMC surface could degrade for a relatively long time period, releasing hydroxyl and Mg^{2+} in a controlled manner. For the PMC samples, the pH value of PMC group with high particle content was higher than that with low particle content. The pH increase also varied among PMCs with the same weight percent of different Mg particles, which should be due to the variation of degradation rate of each Mg particles and their surface fraction in PMCs. For all groups, the pH elevation of solution slowed with prolonged immersion time, indicating the degradation gradually diminishing, which is due to the decrease in metallic Mg on the surface and the protection of degradation products and deposits from solution [30, 35].

The weight changes of PMCs after immersion were also measured (Fig. 3b). Interestingly, the PMCs with higher Mg content showed less weight loss. And the PMCs with “large” pure Mg particles showed the least weight loss, followed by those with “medium” and “small” pure Mg particles. Thus apparently, the weight changes are in reversed trend to the changes of pH value. However, it should be noted that accompanied with the degradation of Mg, part of the degradation products will remain on the samples [37, 38]. Furthermore, CaP products are deposited on sample surface during degradation of Mg [39, 40]. More

intense Mg degradation would lead to higher increase in Mg concentration and pH value in the immersion solution, which further results in more CaP deposition [39, 40]. These contributed to the apparent less decrease or even increase in weight. A number of holes were formed on the surface of PMCs (Fig. 3c), which suggests the degradation or possible detachment of Mg particles. The pore-forming phenomenon was also shown in other kinds of composite bone cement [41] and is beneficial for bone ingrowth and formation of bone/cement physical interlocking. Though with degradation on surface, no significant decrease in the compressive strengths of PMCs was shown (Fig. 3d), which is beneficial for the load-bearing applications.

For biodegradable implant material, the cyto-compatibility of degradation products should be evaluated. Figure 4a shows the O.D. values of MC3T3-E1 pre-osteoblasts when cultured with different extracts for days one and three. At day one, the PMMA extracts group exhibited the best cell growth among the experimental groups, which was also better than the media. The cell growth condition of 0.2-ZK61 and 0.4-ZK61 groups was comparable with the media group, followed by the 0.2-Mg-M, 0.4-Mg-M groups and 0.2-Mg-S, 0.4-Mg-S groups. However, toxicity effect was found for the 0.2-Mg-L, 0.4-Mg-L PMCs (with the O.D. value lower than 75% of the media group), which were prepared with “large” Mg particles. At day three, toxicity effect was also shown for the 0.2-Mg-L and 0.4-Mg-L PMC groups. However, the O.D. values of other PMC groups were larger than those of the PMMA group and comparable to the control group. No significant difference was shown among all the ten groups. Figure 4b shows the pH value of different extracts before cell culture, which indicates that the pH value was increased with increasing particle content for all the PMCs. The samples prepared with “large” Mg particles and ZK61 particles showed the largest and lowest pH increase. Considering the slight difference of pH values among the PMC groups, the toxicity of samples prepared with “large” Mg particles was probably due to the large pH increase and high content of toxic impurity elements in the particles. PMCs that exhibit a good cyto-compatibility have the potential for application in MIOSs.

Figure 5 shows the SEM observation of osteoblast morphologies on the PMMA bone cement and different PMCs after cultured for 1 day. The cells and Mg particles were marked with white and black arrowheads, respectively, while the circular areas with dark color are PMMA particles. First of all, it is clearly shown that osteoblasts on PMCs with lower Mg content exhibited better adhesion and spreading than the cells on PMCs with higher Mg content, which are likely due to more intense gas generation and pH increase in the vicinity of PMCs with higher Mg content. Among the PMCs, samples prepared with “small” Mg

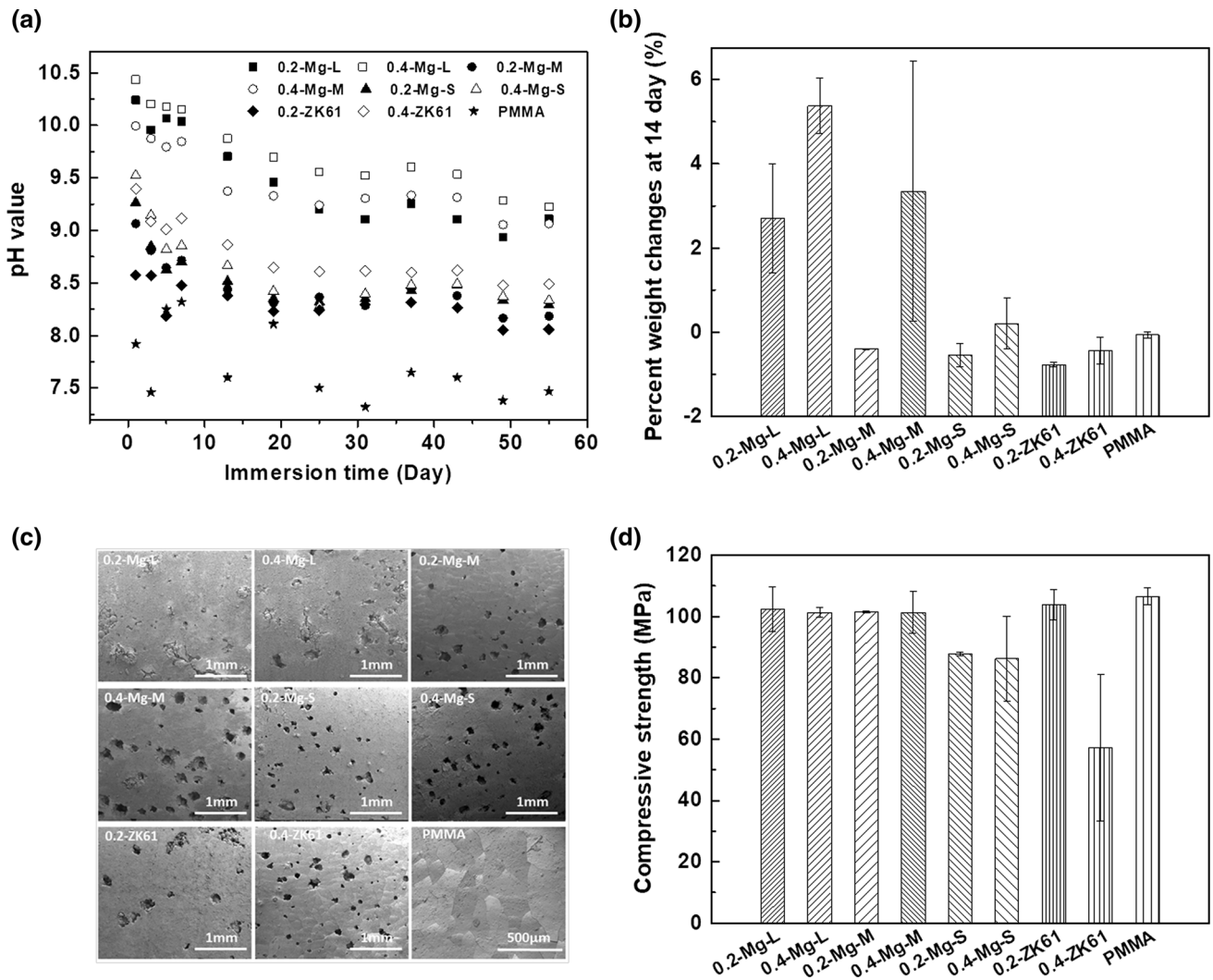


Fig. 3 **a** pH variation of Hanks' solution with cements, **b** percent weight change, **c** typical surface morphology **d** compressive strength of different PMCs after immersion. Data in **a** are shown in means, **b** and **d** are shown in mean \pm standard deviation

particles showed the best cell adhesion and spreading. The adhesion and spreading of osteoblasts on 0.2-Mg-L, 0.2-Mg-M, 0.2-Mg-S, 0.4-Mg-S and 0.2-ZK61 are all better than those on the PMMA, indicating that the addition of Mg particles in a proper manner could promote the surface bioactivity of polymeric materials, which is consistent with the results reported for PCL/Mg hybrid bone substitute [15] and PLGA/Mg alloy composite [16], as well as PMMA/Sr-BG (bioactive glass) [31] and PMMA/quaternized chitosan [33] composite bone cement.

As an injectable and degradable implant material for MIOSs, PMCs should have proper setting, mechanical, degradation and biological properties, all of which are critical for their operation and therapeutic outcomes [24, 34, 42]. Collectively, the results demonstrated that the concentration, particle size and alloy composition of Mg particles affected the setting, mechanical, degradation and

biological properties of PMCs simultaneously and synergistically. Theoretically and as shown by the results, the particle size would affect the injectability, mechanical properties and porous structure after degradation (which is important for ingrowth of bone tissue) of PMCs by altering their setting and rheological properties, and microstructures. Meanwhile, the Mg particles with different sizes may have different degradation rates, which could affect the degradation and biological properties of PMCs. The concentration of Mg particles also affects the physiological, degradation and biological properties of PMCs by influencing the interaction between Mg and PMMA, rheological properties of the mixture during solidification, the microstructure and PMMA/Mg interface area, and the active area fracture on the surface of PMCs after solidification. The composition of Mg particles could also affect all three properties of PMCs by altering the interaction

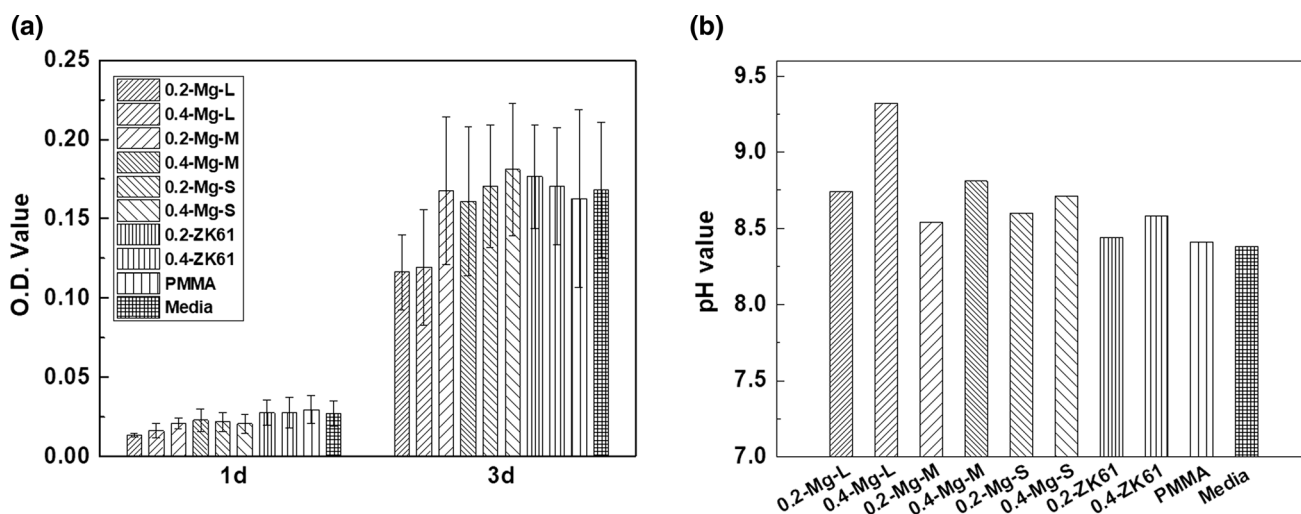


Fig. 4 **a** O.D. values of 96 wells with MC3T3-E1 pre-osteoblasts when cultured with different extracts for one and 3 days. Data are shown in mean \pm standard deviation. One-way analysis of variance was used for statistical analysis. All the pairwise comparisons were made by the post hoc test of Turkey, and no significance was shown at the 0.05 level; **b** pH value of extracts before cell culture in the CCK-8 assay

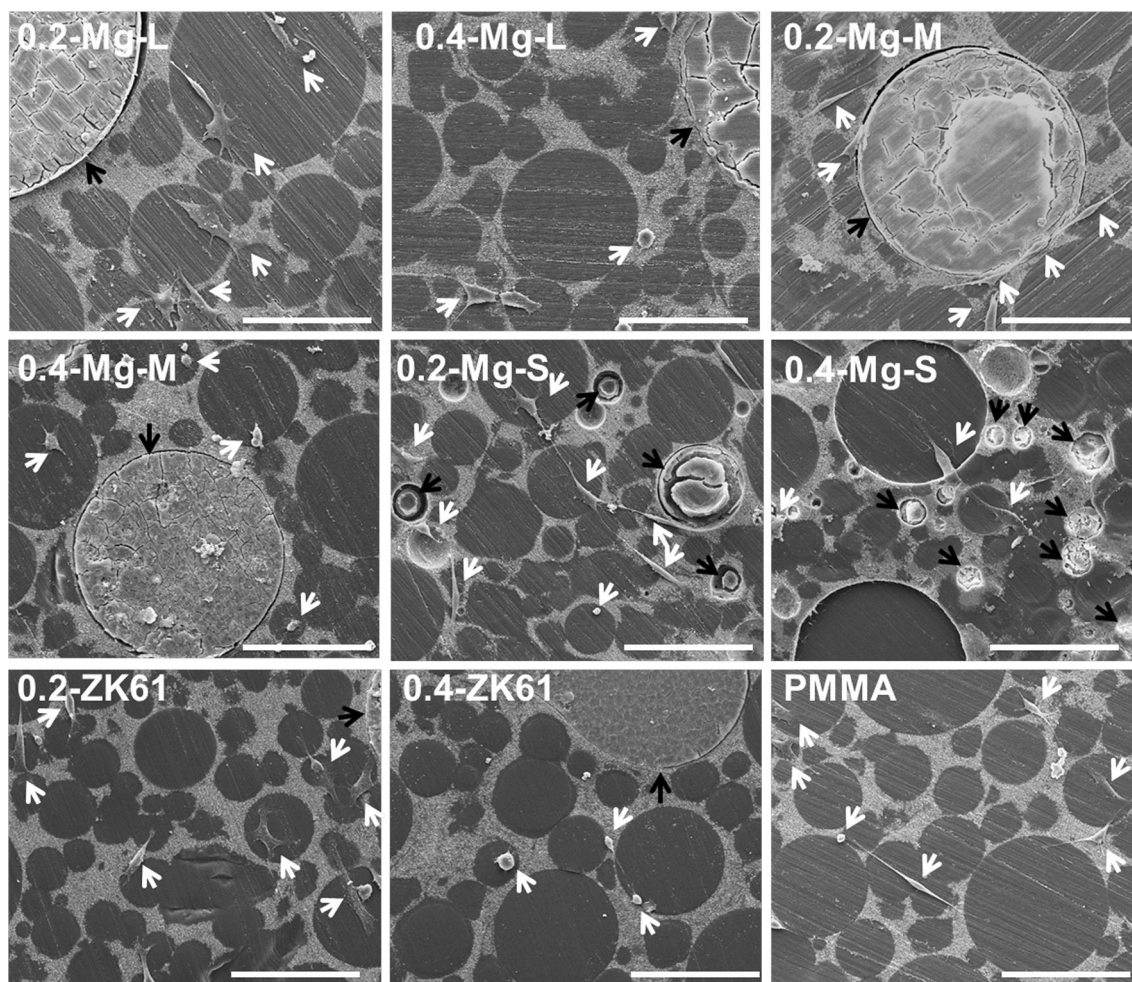


Fig. 5 Morphologies of osteoblasts on the pristine PMMA bone cement and different PMCs after cultured for 1 day. The cells and Mg particles are marked with white and black arrowheads, respectively. Scale bar = 100 μ m

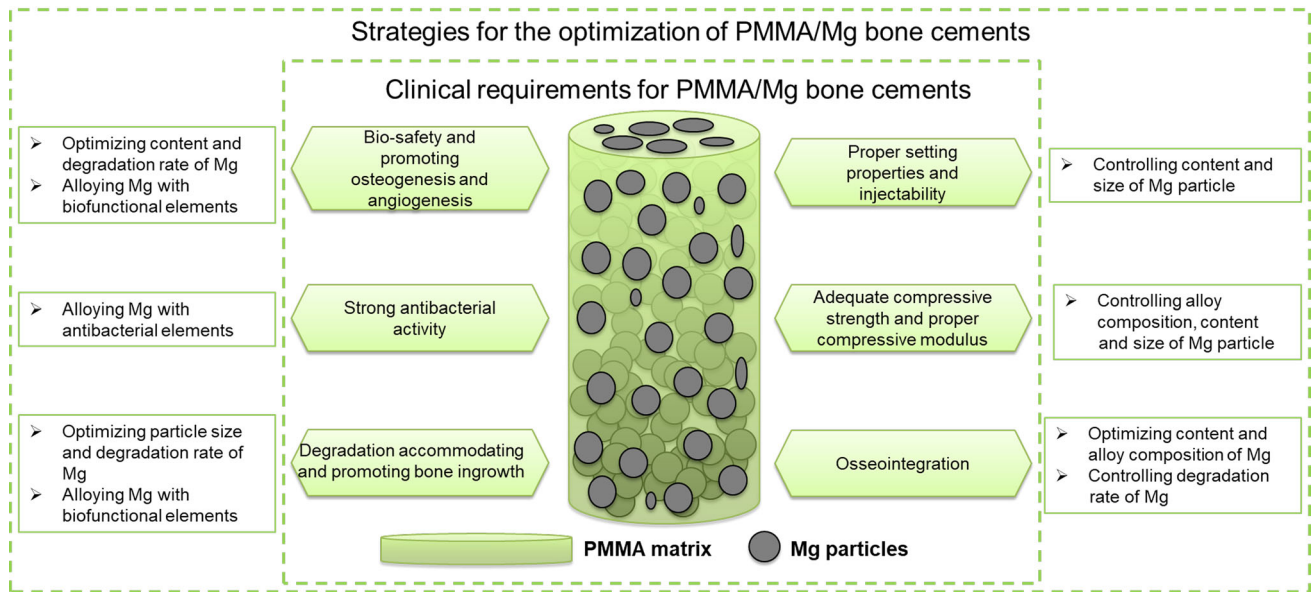


Fig. 6 Clinical requirements for bone cement and the corresponding designing strategies of PMMA/Mg composite bone cements

between Mg and PMMA, the PMMA/Mg interfacial bonding, and the rate/kind of ion released during degradation. Meanwhile, it should be noticed that the influence of one parameter is also dependent on other parameters. For example, the effect of concentration of pure Mg with medium-sized particles on the compressive strength is negligible, while the effect of ZK61 is significant even though they both have the same particles size. Additionally, when increasing the concentration of “large” Mg and “small” Mg within the same range, the compressive strength of the resulting PMCs changed in opposite trends.

The handling properties, mechanical strength, degradation behavior and biocompatibility/bioactivity are four prominent properties of PMC, which are influenced by the concentration, particle size and alloy composition of Mg particles in it. Thus, all the above parameters should be carefully selected to optimize the four properties. Based on the results, the content and size of Mg particles should be well controlled to obtain good injectability. For maintaining good mechanical strength and achieving proper degradation behavior (including proper degradation rate, released products, and resulting morphology), the composition, content, and size of Mg should all be considered. To achieve good biocompatibility/bioactivity, the composition and content of Mg particles should be primarily considered. Figure 6 shows the clinical requirements for bone cement and the corresponding designing strategies of PMCs. Proper content of Mg particles with a selected diameter, composition and degradation rate should be added to achieve good handling, compressive strength and degradation properties. Meanwhile, Mg particles alloyed with bio-functional elements [29, 43–45] should be primarily

considered to endow the PMCs with various bio-functions, such as osseointegration, osteogenic, angiogenic and antibacterial capabilities. Future work will focus on the optimization of PMCs following the strategies proposed in Fig. 6. In vivo evaluation of the tissue response and bonding to PMCs will be performed in order to validate the concept in the future.

4 Conclusion

Partially degradable PMCs were successfully developed and the PMCs degraded and generated porous structures at the surface, while maintaining their original compressive strengths. The injectability, mechanical, degradation and biological properties of the PMCs could be adjusted by controlling the size (within 75–550 μm), alloy composition (pure Mg or ZK61 alloy) and concentration of Mg particles (9–17 wt%). The osteoblast adhesion was enhanced, while the good injectability and compressive strengths of cement were maintained when properly controlling the above parameters. The samples of 0.2-Mg-M and 0.2-ZK61 exhibited the best overall properties among all the PMCs. Collectively, the results showed that the PMCs are promising for application in MIOs and worthy to be further optimized and evaluated.

Acknowledgements This work was supported by the National Natural Science Foundation of China (Nos. 81501858, 81622032, 51501109 and 51672184), the Principal Project of Natural Science Research of Jiangsu Higher Education Institutions (No. 17KJA180011), Jiangsu Innovation and Entrepreneurship Program,

and the Priority Academic Program Development of Jiangsu High Education Institutions (PAPD).

References

- [1] Y.F. Zheng, X.N. Gu, F. Witte, *Mater. Sci. Eng.*, R **77**, 1 (2014)
- [2] X.N. Gu, Y.F. Zheng, *Front. Mater. Sci.* **4**, 111 (2010)
- [3] M.P. Staiger, A.M. Pietak, J. Huadmai, G. Dias, *Biomaterials* **27**, 1728 (2006)
- [4] F. Witte, *Acta Biomater.* **6**, 1680 (2010)
- [5] H. Feng, G. Wang, W. Jin, X. Zhang, Y. Huang, A. Gao, H. Wu, G. Wu, P.K. Chu, *ACS Appl. Mater. Inter.* **8**, 9662 (2016)
- [6] D.A. Robinson, R.W. Griffith, D. Shechtman, R.B. Evans, M.G. Conzemius, *Acta Biomater.* **6**, 1869 (2010)
- [7] J. Liang, R.H. Zhang, Z.J. Peng, B.X. Liu, *Front. Mater. Sci.* **8**, 307 (2014)
- [8] L.Y. Cui, X.H. Fang, W. Cao, R.C. Zeng, S.Q. Li, X.B. Chen, Y.H. Zou, S.K. Guan, E.-H. Han, *Appl. Surf. Sci.* **457**, 49 (2018)
- [9] L.Y. Cui, S.D. Gao, P.P. Li, R.C. Zeng, F. Zhang, S.Q. Li, E.-H. Han, *Corros. Sci.* **118**, 84 (2017)
- [10] R.C. Zeng, L.Y. Cui, K. Jiang, R. Liu, B.D. Zhao, Y.F. Zheng, *ACS Appl. Mater. Inter.* **8**, 10014 (2016)
- [11] Z.Y. Ding, L.Y. Cui, X.B. Chen, R.C. Zeng, S.K. Guan, S.Q. Li, F. Zhang, Y.H. Zou, Q.Y. Liu, *J. Alloys. Compd.* **764**, 250 (2018)
- [12] Y.B. Zhao, L.Q. Shi, L.Y. Cui, C.L. Zhang, S.Q. Li, R.C. Zeng, F. Zhang, Z.L. Wang, *Acta Metall. Sin. (Engl. Lett.)* **31**, 180 (2018)
- [13] J.W. Lee, H.S. Han, K.J. Han, J. Park, H. Jeon, M.R. Ok, H.K. Seok, J.P. Ahn, K.E. Lee, D.H. Lee, S.J. Yang, S.Y. Cho, P.R. Cha, H. Kwon, T.H. Nam, J.H.L. Han, H.J. Rho, K.S. Lee, Y.C. Kim, D. Mantovani, *Proc. Natl. Acad. Sci.* **113**, 716 (2016)
- [14] D. Zhao, S. Huang, F. Lu, B. Wang, L. Yang, L. Qin, K. Yang, Y. Li, W. Li, W. Wang, S. Tian, X. Zhang, W. Gao, Z. Wang, Y. Zhang, X. Xie, J. Wang, J. Li, *Biomaterials* **81**, 84 (2016)
- [15] H.M. Wong, S. Wu, P.K. Chu, S.H. Cheng, K.D.K. Luk, K.M.C. Cheung, K.W.K. Yeung, *Biomaterials* **34**, 7016 (2013)
- [16] Y.H. Cheng, Y.F. Zheng, *J. Mater. Sci. Technol.* **29**, 545 (2013)
- [17] A. Brown, S. Zaky, R.H. Jr, C. Sfeir, *Acta Biomater.* **11**, 543 (2015)
- [18] H.D. Jung, S.P. Hui, M.H. Kang, S.M. Lee, H.E. Kim, Y. Estrin, Y.H. Koh, *Mater. Lett.* **116**, 20 (2014)
- [19] P. Wan, C. Yuan, L. Tan, Q. Li, K. Yang, *Compos. Sci. Technol.* **98**, 36 (2014)
- [20] J. Saleh Khaled, M. El Othmani Mouhanad, H. Tzeng Tony, M. Mihalko William, C. Chambers Monique, M. Grupp Thomas, *J. Orth. Res.* **34**, 737 (2016)
- [21] Z. He, Q. Zhai, M. Hu, C. Cao, J. Wang, H. Yang, B. Li, *J. Orthop. Transl.* **3**, 1 (2015)
- [22] M. Sundfeldt, L.V. Carlsson, C.B. Johansson, P. Thomsen, C. Gretzer, *Acta Orthop.* **77**, 177 (2006)
- [23] G. Lewis, *J. Biomed. Mater. Res. B* **38**, 155 (1997)
- [24] W.F. Mousa, M. Kobayashi, S. Shinzato, M. Kamimura, M. Neo, S. Yoshihara, T. Nakamura, *Biomaterials* **21**, 2137 (2000)
- [25] J.R. Goodheart, M.A. Miller, K.A. Mann, *J. Orthop. Res.* **32**, 1052 (2014)
- [26] S.J. Heo, S.A. Park, H.J. Shin, Y.J. Lee, T.R. Yoon, H.Y. Seo, K.C. Ahn, S.E. Kim, J.W. Shin, *Key Eng. Mater.* **342–343**, 373 (2007)
- [27] C. Wolf-Brandstetter, S. Roessler, S. Storch, U. Hempel, U. Gbureck, B. Nies, S. Bierbaum, D. Scharnweber, *J. Biomed. Mater. Res. B* **101B**, 599 (2013)
- [28] M. Khandaker, Y. Li, T. Morris, *J. Biomech.* **46**, 1035 (2013)
- [29] X. Lin, S. Yang, K. Lai, H. Yang, T.J. Webster, L. Yang, *Nanomed. Nanotechnol. Biol. Med.* **13**, 123 (2017)
- [30] X. Lin, L. Tan, Q. Zhang, K. Yang, Z. Hu, J. Qiu, Y. Cai, *Acta Biomater.* **9**, 8631 (2013)
- [31] I. Goñi, R. Rodríguez, I. García-Arnáez, J. Parra, M. Gurruchaga, *J. Biomed. Mater. Res. B* **106**, 1245 (2017)
- [32] S.B. Kim, Y.J. Kim, T.L. Yoon, S.A. Park, I.H. Cho, E.J. Kim, I.A. Kim, J.-W. Shin, *Biomaterials* **25**, 5715 (2004)
- [33] H. Tan, S. Guo, S. Yang, X. Xu, T. Tang, *Acta Biomater.* **8**, 2166 (2012)
- [34] C. Fukuda, K. Goto, M. Imamura, M. Neo, T. Nakamura, *Acta Biomater.* **7**, 3595 (2011)
- [35] X. Lin, X. Yang, L. Tan, M. Li, X. Wang, Y. Zhang, K. Yang, Z. Hu, J. Qiu, *Appl. Surf. Sci.* **288**, 718 (2014)
- [36] Z. Li, X. Gu, S. Lou, Y. Zheng, *Biomaterials* **29**, 1329 (2008)
- [37] B.J. Wang, D.K. Xu, J.H. Dong, W. Ke, *J. Mater. Sci. Technol.* **34**, 1756 (2018)
- [38] L.Y. Cui, Y. Hu, R.C. Zeng, Y.X. Yang, D.D. Sun, S.Q. Li, F. Zhang, E.-H. Han, *J. Mater. Sci. Technol.* **33**, 971 (2017)
- [39] L. Yang, E. Zhang, *Mater. Sci. Eng., C* **29**, 1691 (2009)
- [40] W.F. Ng, K.Y. Chiu, F.T. Cheng, *Mater. Sci. Eng., C* **30**, 898 (2010)
- [41] S.B. Kim, Y.J. Kim, T.L. Yoon, A.P. Su, I.H. Cho, E.J. Kim, I.A. Kim, J.W. Shin, *Biomaterials* **25**, 5715 (2004)
- [42] G. Lewis, *J. Biomed. Mater. Res. B* **98B**, 171 (2011)
- [43] D. Xia, Y. Liu, S. Wang, R.C. Zeng, Y. Liu, Y. Zheng, Y. Zhou, *Sci. China Mater.* (2018). <https://doi.org/10.1007/s40843-018-9293-8>
- [44] R.C. Zeng, L. Sun, Y.F. Zheng, H.Z. Cui, E.-H. Han, *Corros. Sci.* **79**, 69 (2014)
- [45] C. Shuai, L. Liu, M. Zhao, P. Feng, Y. Yang, W. Guo, C. Gao, F. Yuan, *J. Mater. Sci. Technol.* **34**, 1944 (2018)